Data reduction strategies, uncertainty assessment and resolution of LA–(MC–)ICP–MS isotope data

Matthew S.A. Horstwood

NERC Isotope Geosciences Laboratory

British Geological Survey

Keyworth

Nottingham NG12 5GG

UK

msah@nigl.nerc.ac.uk

1. INTRODUCTION

Publications and interpretations based on isotope analyses of geological and biological materials by laser ablation ICP-MS (including multiple collector and single collector sector field), appear with ever increasing frequency in the scientific literature. The apparent ease and speed with which such data can be gathered lends itself to voluminous production where statistical manipulation and quantity of data can easily mask or become synonymous with quality. Consideration of data corrections and uncertainty estimation combined with known or possible geological/geochemical/analytical phenomena, is crucial to interpreting data appropriately and comprehending the likely resolution of data.

With examples specific to U-Th-Pb geochronology and Hf and Sr isotope geochemistry, data reduction and uncertainty assessment principles will be discussed in order to illustrate likely resolution limits of LA-ICP-MS data in these and other applications.

All data and concepts discussed are based on data acquired using 266nm and 193nm laser ablation systems coupled to MC-ICP-MS instruments and desolvating nebulisers for simultaneous introduction of monitor solutions (see section 2.2).

2. DATA REDUCTION

Having acquired ICP-MS data, either by single collector peak jumping or simultaneous multiple collector methodologies, corrections need to be applied, isotope ratios calculated and uncertainties assessed before the data can be interpreted. This data reduction can take many forms depending on the preference of the analyst, however transparency should be maintained throughout. In general, the less the data need reducing/correcting the fewer the uncertainties that will need propagating and the lower the overall uncertainty. Since the intentions of all are to produce data with the best possible uncertainties, elimination of correction components is therefore more beneficial than correction.

2.1 Laser Induced Elemental Fractionation

Laser induced elemental fractionation (LIEF), where an elemental ratio changes over the course of an ablation, is a common occurrence during single spot static ablation (Fryer *et al*. 1995, Longerich *et al*. 1996) and has been extensively studied and documented for U-Pb geochronology (e.g. Hirata & Nesbitt 1995, Horn *et al.* 2000, Kosler *et al.* 2001). This fractionation is one of the fundamental limiting uncertainties in LA U-Pb geochronology and is a key area of research when trying to improve the precision of the technique.

The usual approach for U-Pb laser ablation analyses is to tolerate LIEF and to correct for this either by assuming that samples and reference materials behave the same, using the same time-slice of data for each (as used in many data processing packages; Horn *et al* 2000) and assuming the normalisation factors are equivalent, or to regress the fractionated response to some initial starting time at which fractionation relative to a standard is assumed to be zero (Sylvester & Ghaderi 1997). However, not all zircons are built the same and any variation of the slope and/or initial fractionation behaviour, can affect the accuracy of the determined result. This variation of the fractionation trend between zircons can be caused through differential U concentrations resulting in metamictisation and/or differential adsorption of the laser energy due to differences in the adsorption characteristics (e.g. colour) of the grains. No single or set of reference material analyses will therefore appropriately normalise out this fractionation which may have its origin in factors other than laser induced effects. The effect on the data will be most apparent when using external normalisation only, where slight differences in matrix between samples and reference materials can cause differences in the required normalisation on the order of a few percent. If selecting a time-slice of the fractionated trend rather than integrating the whole, this effect will be exacerbated and the difference in slope between the reference material and sample will change the apparent concordance of the resultant data point and may lead to selection of a time-slice which renders the data point concordant when in reality it is a truly discordant zircon. The interpretation of this data point will therefore be erroneous since any discordance may not have been along the zero age trajectory caused by LIEF but may instead have reflected a Pb-loss trajectory from a time greater than the apparent age as a result of a later metamorphic event.

When using the intercept method of Sylvester & Ghaderi (1997) these differences in slope and minor matrix effects are largely corrected out but potential differences in the initial normalisation factors may still remain.

Due to the complex nature of these interactions and the resultant greater uncertainty, elimination of LIEF would appear to be beneficial. This can be achieved in two ways – keeping the aspect ratio (depth/diameter) of the ablation pit low (Mank & Mason 1999, Mason & Mank 2001) and/or using a laser with a shorter wavelength (Guillong *et al*, 2003) and/or pulse width (Horn *et al*, this volume). Off-the-shelf 'turn-key' short wavelength and/or short pulse width 213-193nm UV laser ablation systems are now the norm in most laboratories interested in LA geochronology and are capable of excellent results. Laser ablation systems operating with very short femtosecond pulse widths are showing promising results by reducing or eliminating LIEF (see Horn *et al* this volume). Initially however, a more practical solution for most laboratories is to limit the aspect ratio of the ablation crater such that LIEF is reduced to well within analytical uncertainty. Our data indicate that this is only achieved when the aspect ratio is <<1. A typical 213nm or 193nm UV laser system operating with a 25-5ns pulse width ablates an average zircon at c.0.05-0.1μm/pulse using laser fluences of 2-3J/cm2. A 40sec ablation time (first 10secs discarded to allow inter-element ratios to stabilise) at 5Hz equates to a crater depth of c.10-20μm. Using typical spot sizes of 25-50μm this equates to aspect ratios between 0.2-0.8. Figure 1a shows data acquired using just such parameters and indicates fractionation on the order of 10% is still present by the end of the analysis suggesting even smaller depth/diameter ratios are required to eliminate this fractionation altogether when using a static spot.

Using a dynamic ablation pattern (or raster) has been shown to eliminate LIEF in LA U-Pb geochronology (Figure 1b; Horstwood *et al* 2003), apparently reducing significantly any remaining matrix differences and eliminating the need to propagate an additional uncertainty (see comparison of static and dynamic ablation in Kosler *et al*. this volume). However, this benefit is offset by the production of larger ablated particles (Guilloing & Günther, 2001; Günther *et al*; this volume; Kosler *et al*, this volume) which ionise less efficiently in the plasma. However, at the current uncertainty levels of most published U-Pb studies (2-3% 2SD), this does not appear to be limiting. An advantage to the dynamic ablation approach appears to be that some degree of non-matrix matched standardisation can

be achieved (Horstwood *et al*, 2006), reducing the effects of matrix differences between grains of very different chemistry and suggesting a possible way forward in dating less abundant accessory minerals for which homogeneous, accurately calibrated reference materials might not be currently available.

Currently then, an ablation protocol which eliminates LIEF whilst maintaining spatial resolution, precision of the analysis and plasma conditions appears the best way forward for improving the consistency and reliability of U-Pb analyses. In the meantime, the likely constraints imposed by the ablation protocol on the resolution of the data with respect to interpretation, should be considered.

2.2 Monitor solutions

Laser ablation applications typically use a purely dry plasma and sample-standard bracketing protocols to initially tune the system and correct acquired data. Introducing a monitor solution either as a wet or desolvated aerosol, can however help in elucidating any changes in the inter-element fractionation and mass bias of the plasma (Günther *et al.* 1997, O'Connor *et al.* 2006). Initial tuning of the instrument can also be performed more reliably using a stable solution signal rather than the inherently noisy laser ablation signal (Günther *et al.* 1997) and additionally, effects related to variations in the plasma can be separated as distinct from those attributable to the ablation process. Using a monitor solution, many relevant corrections can be performed on-line during the analysis. In this way a more detailed illustration of the various phenomena occurring during each analysis and over the course of an analytical session can be gained. With greater control and understanding of these variables, data reduction procedures can be minimised or altered to cater for these changes and the overall uncertainty for the data reduced. After Longerich *et al* (1987) demonstrated the utility of using the $^{205}Tl/^{203}Tl$ ratio to mass bias correct Pb isotope samples, studies have reported the use of ^{235}U or ^{233}U combined with Tl to elucidate inter-element fractionation effects in the plasma and provide a means of correcting U-Pb data for instrumental mass bias in real time (Horn *et al* 2000, Kosler *et al* 2001; Horstwood *et al* 2003). Comparing these parameters before and during ablation of zircons and monazites using sub-50um spot sizes and a desolvated solution, our data show that inter-element fractionation as monitored by the Tl/U ratio remains constant to within c.0.75% (2SD) and the $^{205}Tl/^{203}Tl$ mass bias is constant to c.0.2% (2SD), suggesting that matrix-induced changes to the plasma are minimal during these ablations.

Figure 2 illustrates this concept using LA U-Pb data acquired in a single session. The data show variation of the inter-element ratio within the plasma as monitored by a simultaneously aspirated $^{205}Tl/^{235}U$ desolvated solution as well as a similar variation in the measured $^{206}Pb/^{238}U$ of the ablated zircon reference material (Figure 2a). Correction of the latter using the former reduces the uncertainty assigned to the Pb/U ratio from c.3.2% (2SD) to c.1% (2SD, Figure 2b), indicating in this instance that much of the inter-element variation experienced during the session is due to plasma instability rather than being related to the ablation process. In essence the monitor solution is being used here as a direct drift correction rather than correcting the resulting data set by mathematical regression. Correcting or at least monitoring the plasma induced inter-element fractionation (PIEF) in this way, also allows the true behaviour of the ablation (e.g. LIEF or lack thereof) to be ascertained. Although the solution behaviour may not be an exact match for that of the ablated material in the plasma, initial correction to the monitor solution provides a reasonable first pass correction which corrects out effects due to variation of the plasma environment, leaving only those effects directly attributable to the ablation and the ionisation of the ablated material. Final normalisation of the data set to an ablation reference material is still required but variations (e.g. fundamental mass bias of the instrument) can be corrected on an integration by integration basis. In this way analytical uncertainty can potentially be improved with the uncertainty propagation for these corrections being effectively 'built in' to the final result since their variations are reflected in the calculations.

A disadvantage of using a monitor solution is that backgrounds are generally increased due to the Pb blank of the acid and spike solutions used, the Pb background within the spraychamber or desolvator and the potential for intermittent spiking of the background. When analysing very small Pb ion beams this can be a significant problem leading to inaccurate data. These disadvantages may however be offset by an increase in overall sensitivity (at least for U-Pb analyses) when utilising a wet plasma (Gehrels *et al*. 2008).

2.3 Complications when interpreting Common-Pb affected data for accessory minerals

Accessory minerals used in U-Pb geochronology commonly contain a modest to significant proportion of non-radiogenic Pb (common-Pb) which is incorporated into the crystal lattice at the time of their crystallisation. This is especially common with monazites (Parrish, 1990) and ubiquitous for other phases such as allanite and titanite. This common-Pb is generally considered to have a composition reflecting the average Pb isotope composition of the host rock which can be determined through the analysis of syngenetic phases. Correction for this component of non-radiogenic Pb is essential in order to determine the true age of the mineral. Without knowledge of the common-Pb composition, one method usually employed to determine this and derive the true age of the mineral is through a Tera-Wasserburg (1972) concordia diagram where correlations to high $^{207}Pb/^{206}Pb$ ratios are interpreted to represent the composition of the common-Pb within the mineral. Regression of this data to determine an intercept age and uncertainty on the Concordia curve (see Figure 3a) then gives the age of the mineral without common-Pb. This approach requires multiple analyses of the same phase in order to define a spread of U-Pb ratios to form the correlation. For individual data points therefore, it is not possible to use this approach unless a $^{207}Pb/^{206}Pb$ composition of the common-Pb component is assumed.

Previous studies have advocated the use of on-line common-Pb corrections (Horstwood *et al* 2003; Storey *et al* 2006), using the calculated ^{204}Pb signal and an assumed common-Pb ratio (e.g. that taken from the Stacey & Kramers (1975) Pb evolution curve at the apparent age of the sample) to directly correct the analysis. Although it is possible to achieve accurate results using this approach, particularly with older mineral grains, it also has its limitations, particularly with young samples where the age of the components contributing the common-Pb can be quite variable. Figure 3 illustrates data from two monazite samples from the Himalaya both of which contain appreciable common-Pb. In Figure 3a data not corrected for common-Pb suggest a correlation between the points with regression to 21Ma and an upper intercept of c.4Ga. However, alternative results and interpretations can be envisaged if the data are considered to represent two groups with similar common-Pb compositions appropriate to the age of the mineral ($^{207}Pb/^{206}Pb$ = 0.837 from Stacey & Kramers (1975) Pb evolution curve at 22Ma, dashed regressions in Fig.3a). Without textural and/or chemical knowledge of the sample grains to provide evidence for the existence of two populations, the interpretation is ambiguous. Figure 3b illustrates another sample where careful chemical mapping and textural relationships have been maintained in

thin section (in the manner advocated by Simonetti *et al*, this volume) such that correlations between equivalent analyses can be seen to define sub-vertical trends on a Tera-Wasserburg plot. Here then the data clearly do not fit a typical common-Pb trend but instead suggest a 'not-so-common' Pb composition with a more vertical trajectory.

Clearly then the exact composition of the common-Pb in a sample can be difficult to predict for on-line correction and as such, assessment and regression of multiple equivalent data points using a Tera-Wasserburg plot appears the best way to proceed unless the composition of the common-Pb component within the sample can be independently determined, e.g. through analyses of feldspar crystals. However, such a determined composition may still be at variance to that recorded in the accessory mineral phases and/or may have been subject to change/alteration. Regardless of whether the common-Pb composition used for correction is measured or assumed, an uncertainty should be assigned and propagated into the final calculation. Mattinson (1987) demonstrated the affect of the common-Pb composition uncertainty on the interpreted $^{207}Pb/^{206}Pb$ age. Appropriate uncertainties for the $^{206}Pb/^{204}Pb$, $^{207}Pb/^{204}Pb$ and $^{208}Pb/^{204}Pb$ ratios can be determined from Stacey & Kramers (1975).

Alternative correction mechanisms use ^{207}Pb or ^{208}Pb to estimate the amount of common-Pb present in the analysis. However, both these approaches assume concordance of the U-Pb and/or Th-Pb systems respectively and so are fundamentally limited in their use. A more useful approach was described by Anderson (2002), deriving a mathematical correction for common-Pb that doesn't rely on the difficult measurement of ^{204}Pb nor assumes concordance. An estimate of the time of lead loss is required but the error arising from uncertainty in this estimate is not limiting.

Another complication is in the use of accessory phases containing common-Pb as reference materials. Here, variable concentrations of common-Pb will lead to variations of the measured $^{206}Pb/^{238}U$ ratio within and between ablations. If this common-Pb is not homogeneously distributed throughout the crystal such that the measured $^{206}Pb/^{238}U$ ratio can be compared to the non-common-Pb corrected reference value, this must first be corrected to determine a true Pb/U normalisation factor by which to correct the unknowns. Inevitably, this must result in a larger uncertainty on the final result when

compared to using a reference material without common-Pb, due to the additional uncertainty of the correction.

Either way, using ICP-MS it is imperative to measure and correct for the ^{204}Hg component of the signal that is inherent to the Ar (and sometimes He) source gas used in plasma mass spectrometry. Monitoring of the Hg-corrected ^{204}Pb component during ablation, with or without direct on-line correction of common-Pb, is essential to be able to ascertain the level of common-Pb which may be affecting an analysis. This is important even for zircons, where micro-inclusions and alteration can result in significant components of common-Pb in the analysis.

2.4 Isobaric Interference Corrections

The above concepts are not restricted to U-Pb isotope ratios. The same principles apply to any inter-element isotope system e.g. Yb-Lu-Hf and Rb-Sr. In these instances however, the accurate determination of inter-element ratios is not generally being attempted, Yb, Lu and Rb having isobars which interfere on one or more of the Hf or Sr isotopes of interest. Accurate on-line correction of these isobars can be achieved by first determining an adapted 'true' ratio for one of the isotope pairs of the interfering element (see full description in Nowell *et al* 2007 and discussion in McFarlane *et al.* this volume). In the case of Rb-Sr for example, the interference free ^{85}Rb peak is used to determine the amount of interfering ^{87}Rb which must be stripped from ^{87}Sr. The ^{87}Rb/^{85}Rb ratio used for this calculation can either be previously determined by mass bias correction using Zr as an adjacent mass element (Waight *et al* 2002) or using Sr itself in a series of experiments at the start of the analytical session where solution reference materials for Sr are doped with Rb to various levels and the adapted 'true' ^{87}Rb/^{85}Rb mass bias corrected ratio calculated using the Sr mass bias assuming ^{86}Sr/^{88}Sr = 0.1194. In this way an adapted ^{87}Rb/^{85}Rb suitable for inversely correcting the Rb isotope ratio during ablation using the Sr mass bias determined at the time, can be determined and accurate on-line interfering element corrections made (Nowell & Parrish 2001; Jackson & Hart 2006).

The same approach can be used for Hf isotope analyses of zircons where ^{176}Yb and ^{176}Lu interfere on ^{176}Hf. Alternatively, a direct measure of the Yb mass bias at the time of ablation can be determined using ^{173}Yb/^{171}Yb (or ^{173}Yb/^{172}Yb, Woodhead *et al* 2004). Indeed, Woodhead *et al* (2004, Fig2b)

illustrate that inaccurately determining the Yb mass bias by c.8% leads to an inaccuracy of 350ppm on the measured $^{176}Hf/^{177}Hf$ ratio. Although differential loading of the plasma on ablation could result in changes in mass bias and inter-element behaviour (O'Connor *et al* 2006), comparison of inter-element and mass bias stability of the plasma before and during ablation using a desolvated Tl/U solution, suggests that for the amount of material typically introduced during laser ablation U-Pb and Hf analyses, inter-element fractionation and mass bias behaviours are essentially constant (see section 2.2). This would suggest that the characterisation of any difference between Hf and Yb mass bias using solution analyses remains stable and consistent during laser ablation analysis. The absolute levels of these biases local to ionising ablation particles could however, be different to those for desolvated solution particles. Inter-element fractionation for example, requires an additional normalisation to an ablation reference material to achieve accurate inter-element data on unknowns. Jackson & Günther (2003) further demonstrated that for volatile elements at least, isotopic fractionation of ablated particles can occur during incomplete vapourisation and ionisation in the plasma. However, our Hf isotope data and that of others (Vervoort *et al*, 2007, Dufrane *et al*, 2007), when compared to chemically purified reference zircons analysed by solution MC-ICP-MS, including those with high REE contents (e.g. R33), indicates that for Hf isotope analysis of zircons, compositions accurate to within c.100ppm can be achieved by laser ablation MC-ICP-MS using Yb correction ratios determined by interferent-doped solution analyses. Clearly, it would currently appear prudent that each laboratory determines the most appropriate methodology for their set-up to achieve accurate results on high-Yb reference materials. Unfortunately, such reference materials are currently limited and/or do not possess the requisite Yb/Hf ratios to prove these corrections to the interference levels seen in some samples. However, the use of multiple standards is encouraged to demonstrate the efficacy of the correction routines at the time of analysis.

For the ^{176}Lu interference correction (and for the Rb-Sr system) direct measurement of two interference-free Lu peaks is not possible since there are only 2 isotopes of Lu. In this case however, the ^{176}Lu correction on ^{176}Hf is so small that an accepted $^{176}Lu/^{175}Lu$ ratio of 0.02653 (or other similar ratios in the literature, e.g. De Bievre, P. & Taylor, P.D.P., 1993) can be used to determine the present day $^{176}Hf/^{177}Hf$ of a zircon, even without allowing for the effect of mass bias on this ratio. However, in order to calculate the Hf isotope ratio at the time of crystallisation, the Lu/Hf inter-element ratio must

be determined accurately in order to correct for the amount of the ^{176}Lu which will have decayed to ^{176}Hf since crystallisation. Here then we have an inter-element ratio which will be affected by both laser and plasma induced elemental fractionation and must be normalised. In this instance, a dynamic ablation pattern or at least an ablation crater with limited aspect ratio will prove beneficial to eliminate any LIEF. A more pressing need however is to have an ablation reference material with a known and constant Lu/Hf ratio such that this normalisation value can be determined. In a natural material such consistency is relatively unlikely and one of the factors currently limiting the total uncertainty on Hf isotope studies of zircons >~500Ma. At present 91500 & BR266 appear to have Lu/Hf ratios consistent to within 10% (Woodhead & Hergt, 2005) and would appear the best options for this purpose. The uncertainty on the Lu/Hf ratio of the reference material, both in terms of the reproducibility experienced during the analytical session and on the reference value, should also be propagated into the calculation of the initial Hf isotope uncertainty (see sections 3.5 & 3.6).

3. UNCERTAINTY ASSESSMENT

To assess the quality of a result for a population of data or a single data point, an uncertainty is required usually expressed at the level of 2sigma (data point) or 95% confidence (population). Proper assessment of the uncertainty of a result is essential. To quote Ludwig (2003), *"… the age of a rock, mineral or process – is unusable in the absence of its uncertainty." "...for most studies, the uncertainty of a date is no less significant than the date itself."* All components of a calculation contribute uncertainties which must therefore be propagated into the final uncertainty. The uncertainty of the result will then reflect the confidence with which this result can be reproduced another time.

For each step of a calculation the uncertainty component must be quantified and its affect on the final result ascertained and propagated into the final uncertainty. This applies both to high precision methodologies of analysis and those of lower precision. Arguably this is even more important for laser ablation methodologies where the size of any correction can vary over orders of magnitude during a single analysis and therefore their associated propagated uncertainties will vary also.

One of the main mechanisms by which isotope results are assessed is through the use of the mean squared weighted deviation (MSWD). This statistical quantity represents the distribution of the data points around the mean value taking into account the data point uncertainties. If MSWD =1 all scatter of the data points can be accounted for as a result of the analytical uncertainties. MSWD values <<1 indicate an overestimation of the data point uncertainties and MSWD values >1 suggest underestimation of the component uncertainties and/or scatter due to non-analytical causes e.g. real geological differences. (For a complete description of the MSWD term see Wendt & Carl 1991). The actual MSWD value for which the scatter of the data can be considered due to analytical factors alone, is not restricted to a value of one but in fact varies according to the number of data points in the calculation (see Fig.3 in Wendt & Carl 1991). So, to be 95% confident that the scatter of the data is due to the analysis when n=5, an acceptable MSWD range would be 0.2-2.2 but for n=25 this would be 0.6-1.5 (see Figure 4). Critically, it should also be noted that MSWD = 1 need not indicate that no geological variation is present, but that any variation is not resolvable at the uncertainty level of the technique used (Kalsbeek 1992).

3.1 Uncertainty propagation

This discussion only attempts to describe the principles by which uncertainty propagation is undertaken and assessed. For comprehensive information on uncertainty estimation and propagation see the EURACHEM/CITAC Guide to Quantifying Uncertainty in Analytical Measurement (http://www.measurementuncertainty.org/mu/guide/index.html).

Uncertainties largely fall into two categories, random (internal) and systematic (external). Random uncertainties are “fluctuations in observations that yield different results each time an experiment is repeated, and thus require repeated experimentation to yield precise results” (Bevington and Robinson, 2003). Assuming that the results are not limited by counting statistics, they should therefore be distributed normally about the mean. Systematic uncertainties are “errors that will make our results different from the “true” values with reproducible discrepancies” (Bevington and Robinson, 2003). These cannot be revealed by repeated measurement (Taylor, 1982) but instead lead to consistent unidirectional inaccuracies in the result. Systematic uncertainties must therefore by identified and eliminated or their size estimated by assessing the determined results against known reference values.

Components of uncertainty are contributed at all levels. Some key components and whether they constitute a random or systematic uncertainty are:

a) Analytical precision of the ratio of interest (random)
b) Analytical precision of the mass bias measurement used for correction (random)
c) Reproducibility (quantified as standard deviation) of corrections for ion counter non-linearity, deadtime and gain relative to a Faraday or other analogue detector system.
d) Reproducibility (standard deviation) of the normalisation factor as determined using the reference material over the course of the analytical session (random)
e) Ability to reproduce a given ratio relative to the size of the smallest isotope signal (random)
f) Uncertainty on the reference value of the primary reference material (systematic)
g) Uncertainty on the correction ratios used (e.g. common-Pb composition, $^{176}Yb/^{173}Yb$, Lu/Hf) (systematic)
h) Uncertainties on decay constants (systematic)

Here then, the reproducibility of the normalisation factor as determined by repeated measurement of the reference material is considered a random uncertainty and is therefore recommended to be propagated into the data point uncertainties of the unknowns and secondary reference materials as advocated by Ireland and Williams (2003). An inaccuracy of the result for the secondary reference material would then constitute a systematic uncertainty the cause of which would need investigating and correcting or quantifying and propagating after assessment of the data populations.

Uncertainties can be propagated using Equation 1:

$$\sigma_z = \sqrt{\left(\frac{\partial Z}{\partial A}\right)^2 .\sigma_A{}^2 + \left(\frac{\partial Z}{\partial B}\right)^2 .\sigma_B{}^2 + \left(\frac{\partial Z}{\partial C}\right)^2 .\sigma_C{}^2} \qquad \text{Equation 1}$$

In this equation each differential term (∂) reflects the partial differential of function Z with respect to one variable, holding all others constant. The partial differentials are then multiplied by the absolute

(not relative) uncertainties for each variable. The uncertainty on Z is equal to the square root of the sum of the squares of all these terms.

By example, the $^{207}Pb/^{235}U$ ratio is often calculated for laser ablation data as:

$$\frac{^{207}Pb}{^{235}U} = \frac{^{207}Pb}{^{206}Pb} * \frac{^{206}Pb}{^{238}U} * 137.88 \qquad \text{Equation 2}$$

The uncertainty propagation for this using Equation 1 is:

$$\sigma_{^{207}Pb/^{235}U} = \sqrt{\left(\frac{^{206}Pb}{^{238}U} * 137.88 * \sigma_{^{207}Pb/^{206}Pb}\right)^2 + \left(\frac{^{207}Pb}{^{206}Pb} * 137.88 * \sigma_{^{206}Pb/^{238}U}\right)^2}$$

Equation 3

However, for some simple forms of uncertainty propagation where corrections relate simply to addition or subtraction of components, e.g. interfering element corrections, Equation 1 can be simplified as Equation 4.

$$\sigma_Z = \sqrt{\sigma_A{}^2 + \sigma_B{}^2 + \sigma_C{}^2} \qquad \text{Equation 4}$$

where $\sigma_{A\text{-}C}$ are the various uncertainty components and must be expressed in relative terms (i.e. as a percentage) and σ_Z is the final propagated uncertainty. Where decay constant and age uncertainties are part of the required uncertainty expression, propagation is most practically carried out by running the 1σ limits through the calculation and propagating this empirically-determined uncertainty envelope by

quadratic addition with the other components of the uncertainty expression as calculated using Equation 1.

The uncertainties thereby defined for $^{206}Pb/^{238}U$ and $^{207}Pb/^{235}U$ are correlated because one is partially derived from the other using a constant $^{238}U/^{235}U$ ratio. This correlation is defined in Equation 5 following Schmitz and Schoene (2007).

$$\rho_{^{206}Pb/^{238}U-^{207}Pb/^{235}U} = \frac{\sigma^2_{207Pb/235U} + \sigma^2_{206Pb/238U} - \sigma^2_{207Pb/206Pb}}{2 * \sigma_{207Pb/235U} * \sigma_{206Pb/238U}} \quad \text{Equation 5}$$

Making the assumption that the $^{207}Pb/^{235}U$ uncertainty results solely from quadratic addition of its two component uncertainties, the correlation coefficient can be simplified as the ratio of the two U-Pb uncertainties derived from rigorous uncertainty propagation (Equations 2 & 3).

$$\rho_{^{206}Pb/^{238}U-^{207}Pb/^{235}U} = \frac{\sigma_{206Pb/238U}}{\sigma_{207Pb/235U}} \quad \text{Equation 6}$$

A fundamental limiting uncertainty is that of the reference material to which the result is being compared or normalised. A result for an unknown sample cannot have an uncertainty better than the reference material to which it is corrected since the uncertainty on the reference material provides the fundamental uncertainty from which the rest of the components are propagated.

Where backgrounds and detector noise are low and correction algorithms are insignificant, uncertainties for measurements taken on very linear and/or sensitive detection systems (e.g. Faraday or ion counting detectors) are limited only by counting statistics: that is, the square root of the total cumulative number of counts per second (N) ratioed against N (equation 7, expressed as a percentage).

$$\frac{\sqrt{N}}{N} * 100 \quad \text{Equation 7}$$

The same principle can however also be applied after all corrections to look at the uncertainty distribution relative to beam size. In this way a minimum uncertainty for an analytical protocol can be determined according to the correction algorithms employed and the size of the ion beam being analysed. For example, Figure 5 illustrates the increase in reproducibility (expressed as 2σ%) of the $^{207}Pb/^{206}Pb$ ratio with decrease in ^{207}Pb as measured on a Faraday detector. The equation there defined can then be used in the uncertainty propagation of the $^{207}Pb/^{206}Pb$ ratio in conjunction with the analysis uncertainty.

The largest uncertainty component for those laser ablation protocols where it exists, is that for calibration of the inter-element ratio. In both U-Pb and Lu-Hf isotope analysis the ability to consistently reproduce the inter-element ratio is limited to the percent level. In the case of Lu-Hf this uncertainty level can reach 10-20% (2SD) depending on the homogeneity of the reference material used, but only becomes a significant factor in the overall uncertainty of the epsilon Hf calculation when high REE concentrations are present and the sample is >c.500Ma. In geochronology studies, the Pb/U uncertainty can normally be reproduced to c.2% 2SD but relies on the assumption that all analyses of the calibration material are concordant (or equally discordant) and equivalent with no variations in Pb/U ratios due to small degrees of Pb-loss, inheritance, etc. Since the Pb/U uncertainty represents the ability to accurately quantify the Pb/U ratio and therefore age at any one time, this uncertainty must be propagated into each data point uncertainty and as such limits the age resolution of a single data point to at least this level. Regardless of whether this is considered a systematic or random uncertainty component, the fact that it is based on reference material data collected with the sample data throughout the analytical session indicates that this uncertainty is relevant at all times to all analyses whether comparing those data collected within or without the same session. The Pb/U uncertainty is therefore, the most significant uncertainty that needs to be controlled to improve age resolution in laser ablation geochronology.

3.2 Secondary and Tertiary reference materials

The limiting uncertainty for any laser ablation study is the ability for the technique to reproduce the data on the reference material used. For most LA studies 2-3 reference materials (or well characterised in-house materials) are generally required – the primary reference material to provide for and quantify

the random uncertainty on any fundamental normalisation and the secondary (and tertiary) to demonstrate accuracy (elucidate any systematic uncertainty) after all corrections, with the different reference materials representing various levels of correction and/or count rates. These secondary and tertiary reference materials can then be used to assess the efficacy of the uncertainty propagation procedure through replicate measurements, i.e. the ability to reproduce a data point after all corrections, appropriate to the analytical routine at the time of analysis. Note that this is still a random uncertainty since the value reproduced might still be inaccurate relative to the true value. Although reference materials with matrices appropriate for quantitative calibration of samples are scarce (Jochum *et al*, this volume), any one reference material can be used to assess the uncertainty level of a protocol through replicate measurements. This may indicate for example that an additional random uncertainty needs propagating due to a difference in the mechanism of ablation for a reference material of a particular kind when compared to the primary.

Figure 6 shows εHf data after all corrections for two zircon reference materials. The first (Fig.6a) has low REE concentrations requiring relatively minor correction of ^{176}Hf for the ^{176}Yb and ^{176}Lu isobaric interferences. Data in Figure 6a are very well constrained with a weighted mean εHf uncertainty of +/- 0.14 (95% conf, absolute) and an MSWD of 1.1. For a sample with high REE (Fig.6b) however, and a ^{176}Hf/^{177}Hf correction >10 times greater than in Figure 6a, the resolution of the result decreases by a factor of three to +/- 0.41 epsilon units (95% conf, absolute) with an MSWD of 2.9 indicating a significant degree of excess scatter. In line with the conclusions of Vervoort *et al* (2007) and Dufrane *et al* (2007), assuming this material is indeed homogenous, this suggests that an uncertainty estimate determined from analyses of more widely available low-REE Hf LA reference materials significantly underestimates the level of propagation required for the higher REE containing materials. Concentrations of these REE may vary during the analysis and the correction routine needs to be responsive and capable of accurately correcting these potentially small-scale variations.

In the example in Figure 7a data for zircon 91500 used as a secondary U-Pb reference material, have been corrected with uncertainty propagated by quadratic addition for the precision of the analysis and the reproducibility of the Plesovice primary reference material. The resulting statistics on a weighted average of the Pb-U age (MSWD = 0.98) suggests that this level of uncertainty propagation is

appropriate and that the variation seen between data points is purely analytical. Should the MSWD prove to be >1, the data can be considered in a probability density plot. If the data are equivalent the distribution will be normal and fall on a single regression line on a linearised probability plot as in Figure 7b. If the data do reflect a normal distribution but result in an MSWD >>1 the data point uncertainties will need reconsidering, suggesting a component has been omitted from the uncertainty propagation. Should the data distribution not be normal, e.g. bimodal, suggesting more than one data population in reality (e.g. geological variation), the material is not clearly one by which to assess the appropriateness of the uncertainty propagation algorithm.

3.3 Use of stable isotope ratios

Interference corrections are often required to achieve the desired data by laser ablation – for example ^{176}Yb and ^{176}Lu corrections on ^{176}Hf, ^{86}Kr and ^{87}Rb corrections on the equivalent sample Sr peaks and ^{204}Hg correction on ^{204}Pb. Where stable isotope ratios are available within the isotope system of interest, interference free or otherwise, they should be calculated after mass bias correction and reported as a measure of data quality. In the Hf isotope system ^{180}Hf/^{177}Hf and/or ^{178}Hf/^{177}Hf should be reported so that data can be viewed with reference to the accuracy of these stable, largely isobar free ratios. Likewise in the Sr isotope system, the ^{84}Sr/^{86}Sr should be reported. These data can then be scrutinised by the independent reader to investigate the underlying robustness of the data with some confidence as to the effect and veracity of the interference correction routines employed for the ^{176}Hf/^{177}Hf and ^{87}Sr/^{86}Sr ratios. Reporting of stable isotope data provides a cross check for any untoward analytical conditions including subtle interferences that may arise during laser ablation, a not uncommon occurrence, and provides the independent observer with confidence as to the quality of the data. Figure 8 illustrates the ^{178}Hf/^{177}Hf stable isotope data for a suite of zircon samples containing various levels of Hf, REE and zirconium from very high to very low. All data indicate a weighted mean ^{178}Hf/^{177}Hf of 1.46723 +/- 7ppm (95% conf, MSWD = 0.53, n=117) with no data points rejected, indicating that relative to an expected ratio of 1.46715 (Patchett & Tatsumoto 1980) the underlying data are robust (since the ^{178}Hf peak requires no corrections except for mass bias).

3.4 Representation of data

Laser ablation ICP-MS is a lower-precision technique than either solution-mode ICP-MS or thermal ionisation mass spectrometry (TIMS). Data produced by disaggregating an inherently heterogeneous solid sample into particles of non-equal size which therefore ionise differently (however slightly) within the plasma, cannot be as precise as data produced by homogenising (i.e. dissolving) and purifying (after chemical separation) the sample material and aspirating it in a controlled fashion as a liquid aerosol (with or without desolvation) into the plasma as a stream of particles of much more equivalent size and composition. For these reasons, solution measurement of dissolved samples purified through ion exchange chromatography, must be more precise than equivalent laser ablation methodologies. Due to the possibility for homogenisation of multiple phases within the sample during dissolution, the question of which technique better reflects the true value is a separate one. However, the uncertainty on the result cannot be better for laser ablation than for an equivalent solution, not least because the initial calibration of a result obtained by laser ablation is often with respect to instrument performance demonstrated through solution analyses and as such this uncertainty provides a limiting uncertainty from which to propagate the laser ablation data.

The laser ablation methodology which possibly comes closest to this is the determination of Hf isotope ratios on zircons. Here, uncertainties of c.0.006% 2SD are quoted (Hawkesworth & Kemp, 2006) for low REE reference materials whilst solution analysis of dissolved and separated aliquots may produce uncertainties of c.0.0015-0.0035% (2SD; Nowell *et al*, 2003). For U-Pb geochronology however, uncertainties of c.2% (2SD) are common for laser ablation compared to c.0.1% for TIMS methodologies, yet final age uncertainties c.10x less can be achieved through the use of weighted mean statistics by virtue of the sheer number of data points (e.g. see Slama *et al.* 2008). The ability for a data point with a 2% uncertainty to resolve a 0.2% difference between itself and its neighbour is very limited. In U-Pb geochronology, instances of minor Pb-loss or inheritance are common and small age differences arising from these sources become irresolvable at the 2% level. A limit of ultimate precision must therefore be admitted in all data with this level being dependent upon the uncertainty level of the data points which define it. According to Ludwig (2008), "…the real limit on accuracy for U/Pb dates is only a factor of two or so better than the analytical error of the individual analyses, rather than amenable to arbitrary improvement by increasing the number of analyses alone. This concept follows statistical limitations on the ability to resolve complexity in the true age structure of a suite of

analyses arising from open system behaviour, presence of xenocrysts, or a variable and non-zero magma-residence-time." Using a high-n dataset to calculate a weighted mean and uncertainty on the result does not therefore indicate the accuracy with which we know the true age but how precisely we know the result defined by that dataset. The statistics assume that all the data are equivalent and fit a normal distribution; this may be the case at the level of 2% data point uncertainties but fine details such as 0.1-0.2% shifts (0.5-1Ma at 500Ma) between data points representing Pb-loss and/or inheritance will not be resolvable (Kalsbeek, 1992) and the existence of such effects breaks the assumption of a single population with normal distribution. Their contribution to the weighted mean or Concordia age calculation (Ludwig, 2003) is however equivalent to the truly concordant data points and in this way can cause the weighted mean result to be biased. If a high-n data set has been collated the difference between the weighted mean age and the true age may be more than the weighted mean uncertainty. Bowring *et al* (2006) compare micro-analytical and TIMS derived data for a sample where minor Pb-loss has resulted in slightly lower Pb/U ratios in the micro-analytical data, but which are masked by the data point uncertainties. Taking the weighted mean statistics on these two datasets results in two ages with uncertainties that don't overlap. This is purely a function of the number of data points used in the weighted mean calculation and is not resolution of a real difference in age.

Therefore, not all data are necessarily the same and should not therefore be included in the same weighted mean calculation. This same argument applies to data at all levels of precision, including ID-TIMS, when dealing with high-n datasets in U-Th-Pb geochronology. Where the data set does conform to a single population with no Pb-loss and/or inheritance effects (e.g. for a reference material), the weighted average of the data set should conform to the result determined by high precision ID-TIMS methodologies and the determined uncertainty will represent the confidence in that value as the average value of the data set. However, the 'limit of interpretation' will still remain as a function limited by the data point uncertainties.

This same principle relates to all ablation data. An analogue can be seen in the laser ablation Hf isotope data shown in Figure 8a where the weighted mean uncertainty of 27 data points is 0.14 epsilon units (=0.0014% or 14ppm!). Any suggestion that this uncertainty represents the confidence in the ability to resolve a result different by 0.003%, is clearly errant and such a suggestion would not be made. Why

then is this practice common when considering age resolution? At some point the limitation of any technique must be admitted and a technique with inherently higher precision capabilities must be used if the resolution of variations much smaller than the data point uncertainties is required.

To this end, when plotting data, fully propagated 2sigma uncertainties should be represented. Use of 1sigma uncertainties conveys undue weight to apparent differences between data points. Figure 9 illustrates this point. The smaller circles represent data points with 1sigma uncertainties, whilst the larger two data points are identical but with 2 sigma uncertainties. The data points with 1 sigma uncertainties could be argued to be significantly different at first inspection but once they are considered with 2 sigma uncertainties it can be seen that they are indistinguishable within this level of uncertainty. To aid objective evaluation of graphically presented data therefore, plotting at the 2sigma level of uncertainty is recommended.

An alternative representation of an uncertainty propagation protocol is given by Gehrels *et al* (2008). Here the major difference is that the author initially excludes the reproducibility of the primary standard on the basis that it is a systematic error and then propagates it later as a standard error with n fixed at 8. This is contrary to the methodology described here and also that of Ireland and Williams (2003) who advocate adding the variance of the reference material to the unknowns.

3.5 Example of uncertainty propagation strategy

The following example illustrates a strategy for the propagation of uncertainties which can be applied across a range of applications. In this example, laser ablation Hf isotope data are propagated by quadratic addition as shown in Equation 4, to calculate a value and uncertainty for epsilon Hf. Results are assessed to investigate whether the uncertainty propagation provides a realistic representation of the true uncertainty.

Example

All data are normalised to the average of pure and Yb-doped JMC475 Hf solution reference material analyses (using a $^{176}Hf/^{177}Hf$ value of 0.282160, Patchett & Tatsumoto 1980) run to assess instrumental performance and to determine the Yb correction. Zircon reference material Mud Tank (U-Pb age 732

+/- 5Ma, Black & Gulson 1978, $^{176}Hf/^{177}Hf$ = 0.282507, Woodhead & Hergt 2005) is used to assess accuracy of laser ablation results after normalisation to the JMC475 results. Sample $^{176}Hf/^{177}Hf$ analytical uncertainties are propagated with the reproducibility of the Mud Tank reference material. 91500 is used as the primary standard for normalisation of the Lu-Hf inter-element fractionation with reference to the values of Woodhead & Hergt (2005). Sample Lu-Hf uncertainties are propagated with the session reproducibility for the Lu-Hf ratio of 91500 or the variation of the Lu/Hf ratios known to occur in the reference material (whichever is greatest). Finally the 2σ age uncertainty is considered also, as determined by TIMS, SIMS or LA. The age uncertainty used should relate to the age quoted, i.e. if only a single spot $^{206}Pb/^{238}U$ or $^{207}Pb/^{206}Pb$ age has been determined, the single spot uncertainty propagated with reference to the U-Pb standard, should be used. If a full multi-point Concordia age determination has been used to calculate the age, this final age uncertainty should be used. In this way, some of the uncertainty as to the known age of the sample/analysis will be built into the uncertainty for epsilon Hf.

An example set of data used for these calculations is shown below.

Uncertainty component (random)	*$^{176}Hf/^{177}Hf$*	*2SD*
Yb doped and non-doped solution JMC475	0.282145	0.0039%
Mud Tank (after norm to JMC475)	0.282509	0.0090%
Sample precision (after norm to JMC475)	0.282495	0.0099% (2SE), 0.0139% (2σ) after propagation

Uncertainty component (random)	*$^{175}Lu/^{177}Hf$*	*2SD*
91500 (including 2SD of Lu/Hf external variation)	0.000313	9.6%
Sample (after norm to 91500 Lu/Hf)	0.000145	0.36% (2SE) 9.6% (2σ) after propagation

Uncertainty component (systematic)	*Age*	*2SD*
TIMS, SIMS or LA age of sample	337Ma	1Ma

Epsilon Hf calculation	-2.13	1.44
(c.f. Epsilon Hf Population (uncertainty at 2SD)	-2.4	1.11)
(wtd mean of population (MSWD = 0.51, n = 20)	-2.37	0.34)

The resulting MSWD suggests that there may be a small component of overestimation in this propagation strategy.

3.6 Effect of U-Pb age discordance and uncertainty on εHf.

The effect of the sample age uncertainty on the final epsilon Hf uncertainty should also be considered. Figure 10a plots data for four samples between 337-2000Ma, with $^{176}Yb/^{177}Hf$ and $^{176}Lu/^{177}Hf$ ratios ranging between 0.0042-0.0407 and 0.00004-0.00049 respectively. Varying the age uncertainty from 1-20Ma for these samples, whilst keeping all other variables constant, increases the uncertainty on the epsilon Hf value by c.50%. A bias in εHf can also be seen with respect to discordance. Quantification of discordance for detrital zircon samples is usually based on the percentage distance of the data point along a Discordia through the origin to the upper intercept, in essence the percentage difference between the determined $^{207}Pb/^{206}Pb$ and $^{206}Pb/^{238}U$ ages. If the apparent Pb-loss from the grain was only a recent phenomenon, the Pb-Pb age represents the true age and there will be no bias in the determination of the εHf value from this grain regardless of the amount of Pb-loss suffered. If however, Pb-loss was an ancient phenomenon, the Pb-Pb age represents only a minimum age and even though the $^{206}Pb/^{238}U$ age might only be 5% discordant relative to the $^{207}Pb/^{206}Pb$ age, the true age of this grain will be older. In this instance, a Hf isotope determination on a 'relatively concordant' grain, could still represent a significant bias from the true εHf value. This is shown in Fig 10b which shows the variation of calculated εHf as a result of using the $^{207}Pb/^{206}Pb$ upper intercept age of a discordant zircon that has experienced ancient Pb-loss. Relative to the true age of 2Ga, the calculated εHf may show a bias of up to c.1.5 εHf for a 5% discordant grain resulting from c.17% Pb-loss at 1Ga. A similar grain that has only suffered 10% Pb-loss at 1Ga will appear 2.9% discordant, i.e. pretty much concordant within the uncertainties of a large proportion of LA U-Pb data, but will still show a bias of 0.85 in the calculated εHf using the determined $^{207}Pb/^{206}Pb$ age. Note that this is still outside of the uncertainties reported for most LA Hf isotope data.

Considering the demonstrated effect of both the age uncertainty and discordance in the interpretation of the true age, a discordant data point not overlapping Concordia has a large uncertainty in determining both the true age and the relevant age uncertainty and this should be reflected in both the calculation of epsilon Hf uncertainty (see Fig.10a) and the potential for bias in the εHf value (Fig. 10b). In practice, due to the non-linear nature of the age equations, these uncertainties will be asymmetric. For Hf isotope determinations on detrital zircons therefore, datapoint age uncertainties should be used in the calculation of individual epsilon Hf uncertainties for each analysis and these analyses are best conducted only on those data points well within uncertainty of the U-Pb Concordia.

4. SUMMARY

The approach outlined above highlights an empirical approach for assessing the uncertainty of laser ablation isotope data. Although focussing on the U/Pb, Hf and Sr isotope systems this approach is valid for other systems and has been used in assessing uncertainty contributions in other studies (e.g. depleted uranium solution analysis of chemically separated urines, Parrish *et al*, 2008).

On-line monitoring and real-time correction of data helps elucidate competing phenomena, reduces off-line data reduction of data averages and includes relevant uncertainty components, whilst elimination of variable components of uncertainty (e.g. LIEF) also limits the necessity for uncertainty propagation.

Secondary and Tertiary reference materials or other ‘knowns’ can be used extensively to investigate the reproducibility of analytical protocols, accuracy and long term performance and in deriving the uncertainty propagation protocol required. Results from these secondary reference materials can then be used on a per session basis to validate the data at the time. Quotation of stable isotope data is strongly encouraged, to indicate the underlying robustness of the fundamental corrections applied to all the data when inaccuracy of other ratios of interest might reflect poor performance of additional isobaric or other interference corrections performed at the time.

All data should be graphically presented and interpreted at the 2σ level and the limit of interpretation, reflected largely by the data point uncertainties, should be appreciated and respected without recourse to statistical manipulation of high-n datasets. The benefit of laser ablation resides in the ability to resolve different components to relatively high spatial resolution. However, it is a relatively low-precision technique and its benefits are undermined when undue weight of interpretation is placed on data whose precision has been statistically enhanced. Low-precision data may reflect a normal distribution with MSWD values ~1 but can hide and not resolve, small-scale variations which break the fundamental assumption of a normal distribution. These non-equivalent data can then result in inaccurate results when included in weighted mean statistical assessments. Higher precision methodologies should therefore be employed where a higher level of precision is required.

The effect of a component uncertainty from one isotope system on the calculations and uncertainties of another should not be forgotten and can be a significant factor limiting the resolution of data and its interpretation.

Acknowledgements

My many thanks go to visiting Professor Jon Patchett and my NIGL colleagues Steve Noble, John Cottle, Dan Condon and Randy Parrish for their comments and time in discussing and elucidating the various aspects in this paper. Many thanks are also due to Tom Anderson and George Gehrels for their constructive reviews.

References

ANDERSON, T. (2002): Correction of common lead in U–Pb analyses that do not report ^{204}Pb. *Chem. Geol.*, **192**, 59-79

BEVINGTON, P.R. & ROBINSON, D.K. (2003): Data reduction and error analysis for the physical sciences. 3rd Edition. McGraw-Hill, New York.

BLACK, L.P. & GULSON, B.L. (1978): The age of the Mud Tank Carbonatite, Strangways range, Northern Territory. *BMR Journal of Australian Geology and Geophysics* **3**, 227–232.

BOWRING , S.A. , SCHOENE, B., CROWLEY , J.L, RAMEZANI, J. & CONDON, D.J. (2006): High-precision U-Pb geochronology and the stratigraphic record: progress and progress. 25-46. *In* Geochronology, Emerging Opportunities. (T. D. Olszewski, ed.) *The Paleontological Society Spec. Pub*., *vol.* **12**, New Haven.

COTTLE, J.M. (2007): Timing of crustal metamorphism, melting and exhumation of the Greater Himalayan, crust, Makalu-Kangshung-Kharta region, South Tibetan Himalaya. PhD Thesis, University of Oxford.

DE BIEVRE, P. & TAYLOR, P.D.P. (1993): Table of the isotopic composition of the elements. *Int. J. Mass Spectrom. Ion Process.* **123**, 149.

DUFRANE S.A., VERVOORT, J.D., AND HART, G.L., (2007): Uncertainty of Hf isotope analysis in zircon using LA-MC-ICPMS techniques: Full disclosure. 17th Annual V.M. Goldschmidt Conference, Cologne, Germany, August 2007, Geochim. et Cosmochim. Acta, v. 71 (15), p. A241.

EURACHEM/CITAC Guide (2000): Quantifying Uncertainty in Analytical Measurement. 2nd Edition. Eds S L R Ellison, M Rosslein, A Williams. ISBN 0 948926 15 5. LGC Information Services, Middlesex, UK. http://www.measurementuncertainty.org/mu/guide/index.html

FOSTER, G., GIBSON, H.D. PARRISH, R.R., HORSTWOOD, M., FRASER, J. & TINDLE, A. (2002): Textural, chemical and isotopic insights into the nature and behaviour of metamorphic monazite. *Chemical Geology*, **191**, 183– 207

FRYER, B.J., JACKSON, S.E. & LONGERICH, H.P. (1995): The design, operation and role of the laser ablation microprobe coupled w ith an inductively coupled plasma mass spectrometer (LAM-ICP-MS) in the earth sciences. *Can. Min.*, **33**, 303-312

GEHRELS, G.E., Valencia, V.A. & Ruiz, J. (2008): Enhanced precision, accuracy, efficiency, and spatial resolution of U-Pb ages by laser ablation-multicollector-inductively couple plasma-mass spectrometry. *Geochemistry, Geophysics, Geosystems*, **9**, no.3.

GREGORY, C.J., RUBATTO, D., ALLEN, C.M., WILLIAMS, I.S., HERMANN, J. & IRELAND, T. (2007): Allanite micro-geochronology: a LA-ICP-MS and SHRIMP U-Th-Pb study. Chem. Geol., doi: 10.1016/j.chemgeo.2007.07.029

GUILLONG, M. & GÜNTHER, D. (2002): Effect of particle size distribution on ICP-induced elemental fractionation in laser ablation-inductively coupled plasma-mass spectrometry. *J. Anal. At. Spectrom.*, **17**, 831-837

GUILLONG, M., HORN, I. & GÜNTHER, D. (2003): A comparison of 266nm, 213nm and 193nm produced from a single solid state Nd:YAG laser for laser ablation ICP-MS. *J. Anal. At. Spectrom.*, **18**, 1224–1230

GÜNTHER, D. & KOCH, J. (2008): Formation of aerosols generated by laser ablation and their impact on elemental fractionation in LA-ICP-MS. *Mineralogical Association of Canada Short Course Series Volume*, **40**, xx-xx (this volume).

GÜNTHER, D., COUSIN, H., MAGYAR, B. & LEOPOLD, I. (1997): Calibration studies on dried aerosols for laser ablation-inductively coupled plasma mass spectrometry. *J. Anal. At. Spectrom.*, **12**, 165-170

HAWKESWORTH, C.J. & KEMP, A.I.S. (2006): Using hafnium and oxygen isotopes in zircons to unravel the record of crustal evolution. *Chemical Geology*, **226**, 144–162.

HIRATA, T. & NESBITT, R.W. (1995): U-Pb isotope geology of zircon: Evaluation of the laser probe-inductively coupled plasma mass spectrometry technique. *Geochimica et Cosmochimca Acta*, **59**, 2491-2500.

HORN, I., MCDONOUGH, W.F. & RUDNICK, R.L. (2000): Precise elemental and isotope ratio determination by simultaneous solution nebulisation and laser ablation ICP-MS: Application to U/Pb geochronology. *Chemical Geology*, **167**, 405-425

HORN, I. (2008): Comparison of femtosecond and nanosecond laser interactions with geologic matrices and their influence on accuracy and precision of LA-(MC)-ICPMS data. *Mineralogical Association of Canada Short Course Series Volume*, **40**, xx-xx (this volume).

HORSTWOOD, M.S.A., FOSTER, G.L., PARRISH, NOBLE, S.R. & NOWELL, G.M. (2003): Common-Pb correction in-situ U-Pb accessory mineral geochronology by LA-MC-ICP-MS. *J. Anal. At. Spectrom.*, **18**, 837-846.

HORSTWOOD, M.S.A., PARRISH, R.R., CONDON, D.J. & PASHLEY, V. (2006): Laser ablation acquisition protocols and non-matrix matched standardisation of U-Pb data. *Geochimica et Cosmochimica Acta*, **70**, No.18, Supplement 1, A264.

IRELAND, T.R. & WILLIAMS, I.S. (2003): Considerations in Zircon Geochronology by SIMS. *In* Zircon (Hanchar, J.M. & Hoskin, P.W.O. eds.) *Reviews in Mineralogy & Geochemistry, Volume 53*, 215-238.

JACKSON, M.G. & HART, S.R. (2006): Strontium isotopes in melt inclusions from Samoan basalts: Implications for heterogeneity in the Samoan plume**.** ***Earth and Planetary Science Letters,*** 245 **260–277**

JACKSON, S.E. & GÜNTHER, D. (2003): The nature and source of laser induced isotopic fractionation in laser ablatio-multicollector-inductively couple plasma-mass spectrometry. *J. Anal. At. Spectrom.*, **18**, 205-212

JOCHUM, K. & STOLL, B. (2008): Reference materials for elemental and isotopic analyses by LA-(MC-)ICP-MS: successes and outstanding needs. *Mineralogical Association of Canada Short Course Series Volume*, **40**, xx-xx (this volume).

KALSBEEK, F. (1992): The statistical distribution of the mean squared weighted deviation – Comment: Isochrons, errorchrons, and the use of MSWD-values. *Chem. Geol.*, **94**, 241-243.

KOSLER, J., TUBRETT, M & SYLVESTER, P.J. (2001): Application of laser ablation ICP-MS to-U-Th-Pb dating of monazite. *Geostandards Newsletter*, **25**, No.23, 375-386.

KOSLER, J. (2008): Laser ablation sampling strategies for concentration and isotope ratio analyses by ICP-MS. *Mineralogical Association of Canada Short Course Series Volume* **40**, xx-xx (this volume).

LONGERICH, H.P, FRYER, B.J. & STRONG, D.F. (1987): Determination of lead isotope ratios by inductively coupled plasma mass spectrometry (ICP-MS). *Spectrochimica Acta* **42B**, 39-48.

LONGERICH, H.P, GÜNTHER, D. & JACKSON, S.E. (1987): Elemental fractionation in laser ablation inductively coupled plasma mass spectrometry. *Fres. Jour. Anal. Chem.* **355**, 538-542

LUDWIG, K.R. (2003): Mathematical-Statistical Treatment of data and errors for ^{230}Th/U geochronology. In Uranium Series Geochemistry (Bourdon *et al*, eds) Reviews in Mineralogy and Geochemistry, Mineralogical Society of America, Volume 52, 631-656.

LUDWIG, K.R. (2008): User's Manual for Isoplot 3.6, A Geochronological Toolkit for Microsoft Excel. Berkeley Geochronology Center Special Publication No. 4

MANK, A.J.G. & MASON, P.R.D. (1999): A critical assessment of laser ablation ICP-MS as an analytical tool for depth analysis in silica-based depth analysis. *J. Anal. At. Spectrom.*, **14**, 1143-1153.

MASON, P.R.D. & MANK, A.J.G. (2001): Depth-resolved analysis in multi-layered glass and metal materials using laser ablation inductively coupled plasma mass spectrometry (LA-ICP-MS) *J. Anal. At. Spectrom.*, **16**, 1381–1388.

MATTINSON, J.M. (1987): U-Pb ages of zircons: A basic examination of error propagation. *Chem. Geol.*, **66**, 151-162.

NOWELL, G.M. & PARRISH, R.R. (2001): Simultaneous acquisition of isotope compositions and parent/daughter ratios by non-isotope dilution-mode plasma ionisation multi-collector mass spectrometry (PIMMS). *In* Plasma Source Mass Spectrometry: The New Millenium (Holland, G. & Tanner, S.D.) *Royal Soc. Chem.,Spec. Publ.* **267**, 298-310

NOWELL, G.M., PEARSON, D.G., PARMAN, S.W., LUGUET, A. & HANSKI, E. (2007): Precise and accurate $^{186}Os/^{188}Os$ and $^{187}Os/^{188}Os$ measurements by Multi-Collector Plasma Ionisation Mass Spectrometry, part II: Laser ablation and its application to single-grain Pt-Os and Re-Os geochronology. *Chem. Geol*., **248**, 394–426.

NOWELL, G.M., PEARSON, D.G., OTTLEY, C.J., SCHWIETERS, J & DOWALL, D. (2003): Long-term performance characteristics of a plasma ionisation multi-collector mass spectrometer (PIMMS): The ThermoFinnigan Neptune. *In* Plasma source Mass Spectrometry: Applications and emerging technologies. (Holland, G. & Tanner, S.D. eds), *Royal Soc. Chem*. Cambridge, UK.

O'CONNOR, C., SHARP, B.L. & EVANS, P. (2006): On-line additions of aqueous standards for coalbration of laser ablation inductively coupled plasma mass spectrometry: theory and comparison of wet and dry plasma condictions. *J. Anal. At. Spectrom.*, **21**, 556-565.

PARRISH, R.R. (1990): U-Pb dating of monazite and its application to geological problems. *Can. J. Earth Sci*., **27**, 1431-1450.

PARRISH, R.R., HORSTWOOD, M., ARNASON, J.G., CHENERY, S., BREWER, T., LLOYD, N.S. & CARPENTERD.O. (2008): Depleted uranium contamination by inhalation exposure and its detection after ~20 years: implications for health assessment. *Sci. Total. Env.* **390**, 58-68.

PATCHETT & TATSUMOTO (1980): A routine high-precision method for Lu-Hf isotope geochemistry and chronology. Contribs. Min. Pet., 75, 263-267.

SCHMITZ, M.D. & SCHOENE, B. (2007): Derivation of isotope ratios, errors, and error correlations for U-Pb geochronology using ^{205}Pb-^{235}U-(^{233}U)-spiked isotope dilution thermal ionisation mass spectrometric data. *Geochemistry, Geophysics, Geosystems*, **8**, No.8.

SIMONETTI, A., HEAMAN, L.M. & CHACKO, T. (2008): Use of discrete-dynode secondary electron multipliers with Faradays – A '*reduced volume'* approach for *in-situ* U-Pb dating of accessory minerals within petrographic thin section by LA-MC-ICP-MS. *Mineralogical Association of Canada Short Course Series Volume*, **40**, xx-xx (this volume).

SLÁMA, J., KOŠLER, J., CONDON, D.J., CROWLEY, J.L., GERDES, A., HANCHAR, J.M., HORSTWOOD, M.S.A., MORRIS, G.A. & NASDALA, L., NORBERG, N., SCHALTEGGER, U., SCHOENE, B., TUBRETT, M.N., WHITEHOUSE, M.J. (2008): Plešovice zircon — A new natural reference material for U–Pb and Hf isotopic microanalysis. *Chem. Geol.*, **249**, 1-35

STOREY, C.D., JEFFRIES, T.E. & SMITH, M. (2006): Common lead-corrected laser ablation ICP–MS U–Pb systematics and geochronology of titanite. *Chemical Geology*, **227**, 37– 52

STACEY, J.S. & KRAMERS, J.D. (1975): Approximation of terrestrial lead isotope evolution by a two-stage model. *Earth and Planet. Sci. Lett.*, **26**, 207-221.

SYLVESTER, P.J. & GHADERI, M. (1997): Trace element analysis of scheelite by excimer laser ablation inductively coupled plasma mass spectrometry (ELA-ICP-MS) using a synthetic silicate glass standard. *Chemical Geology*, **141**, 49-65.

TAYLOR, J.R. (1982): *An introduction to error analysis: the study of uncertainties in physical measurements.* University Science Books, CA, USA.

TERA, F. & WASSERBURG, G.J. (1972): U-Th-Pb systematics in three Apollo 14 basalts and the problem of intial Pb in lunar rocks. *Earth. Planet. Sci. Lett*, **17**, 281-304.

VERVOORT, J., DUFRANE, S., AND HART, G., (2007): An assesment of the total uncertainty in Hf isotope analyses by LA-MC-ICPMS, Eos Trans. AGU, v. 87, Fall Meet. Suppl., Abstract V51B-0569.

WAIGHT, T., BAKER, J. & WILLIGERS, B. (2002): Rb isotope dilution analyses by MC-ICPMS using Zr to correct for mass fractionation: towards improved Rb–Sr geochronology? *Chem. Geol.* **186**, No.1-2, 99-116

WENDT, I. & CARL, C. (1991): The statistical distribution of the mean squared weighted deviation. *Chem. Geol.*, **86**, 275-285.

WOODHEAD, J., HERGT, J., SHELLEY, M., EGGINS, S. & KEMP, R. (2004): Zircon Hf-isotope analysis with an excimer laser, depth profiling, ablation of complex geometries, and concomitant age estimation. *Chem. Geol.*, **209**, 121-135

WOODHEAD, J.D. & HERGT, J.M. (2005): A preliminary appraisal of severn natural zircon reference materials for in situ Hf isotope determination. Geostandards and *Geoanalytical Research*, **29**, No.2 183-195.

Figure captions

Figure 1 – Comparative laser-induced inter-element fractionation (LIEF) during a) static ablation and b) dynamic ablation

Figure 2 – Variation of plasma-induced inter-element fractionation (PIEF) during an analytical session a) measured ratios for both desolvated solution aspiration ($^{205}Tl/^{235}U$) and laser ablation ($^{206}Pb/^{238}U$) for a number of analyses. Ratio variation is *c.*3.2% 2SD b) $^{206}Pb/^{238}U$ of the same analyses after normalisation to $^{205}Tl/^{235}U$. Ratio variation is *c.*1% 2SD

Figure 3a – Tera-Wasserburg plot illustrating different common-Pb interpretations for a c.20Ma monazite sample. Dashed lines are possible common-Pb regression trajectories for different parts of the data. Solid line is a linear regression of all the data using Isoplot (Ludwig, 2008).

Figure 3b – Monazite sample recording various growth events all with a 'not-so-common' common-Pb composition. Ages on the left of the diagram are calculated using $^{207}Pb/^{206}Pb = 0.86$, ages on the right are the weighted average $^{206}Pb/^{238}U$ age of the data points constituting each population. (data taken from Cottle, 2007)

Figure 4 – Range of acceptable MSWD values when scatter of data can be considered due to analytical causes alone (data distilled from fig. 3. Wendt & Carl 1991)

Figure 5 – $^{207}Pb/^{206}Pb$ ratio reproducibility as determined using reference zircons and multiple ion counters, relative to the count rate of ^{207}Pb. The determined relationship can then be used to propagate an appropriate level of uncertainty for each sample data point based upon the count rate of ^{207}Pb in the analysis.

Figure 6a – εHf data for a low REE Hf isotope reference material. Note MSWD ~1 indicating appropriate uncertainty propagation.

Figure 6b – εHf data for a high REE Hf isotope reference material. Note MSWD >>1 indicating data point uncertainties require expansion (or reference material is not homogeneous)

Figure 7a – Pb/U age data (static ablation) for 91500 zircon normalised to Plesovice zircon. Data acquired over c.6 months. Grey box represents uncertainty of +/-1.5% (2SD).

Figure 7b – Data for 7a showing a normal distribution and as a linearised probability plot both indicating a single homogeneous population at the resolution of the input data point uncertainties.

Figure 8 – $^{178}Hf/^{177}Hf$ data for a range of Hf isotope reference materials with low to high REE interference corrections. Reporting of such stable isotope data along with the radiogenic data of interest is considered essential in order to illustrate the underlying data quality.

Figure 9 –1σ vs 2σ data point uncertainties illustrating the degree of overlap and therefore potential equivalence when considered at 2σ. At 1σ the potential for data points to be equivalent might not be recognised, leading to spurious interpretation of differences.

Figure 10a – The effect of increased age uncertainty on calculated εHf uncertainty

Figure 10b – The difference in the calculated εHf between apparent ($^{207}Pb/^{206}Pb$ intercept) age and true age for a discordant 2Ga zircon. The effect of different percentages of ancient Pb-loss are illustrated. A detrital zircon with an apparent 5% discordance (i.e. Pb-loss trajectory through zero) at the present time, but which suffered up to c.15% pb-loss at 1Ga, will result in a bias in the calculated εHf of c. -1.3. Zircons only affected by modern-day Pb-loss or igneous populations whose true age can be determined through regression will not show this bias.

Figures

Figure 1a

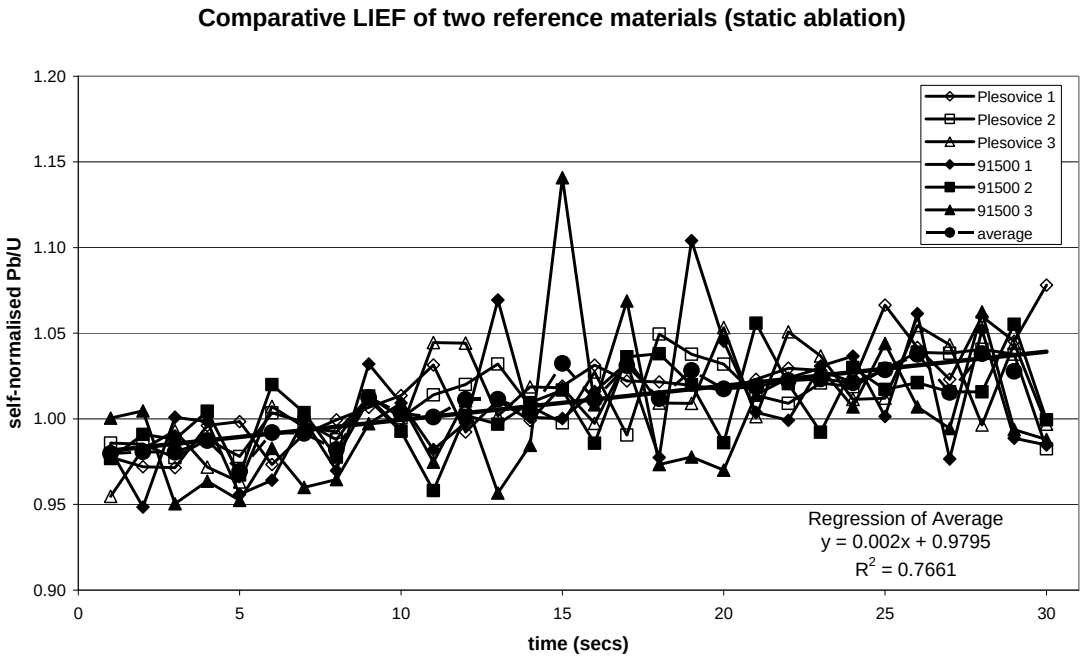

Figure 1b

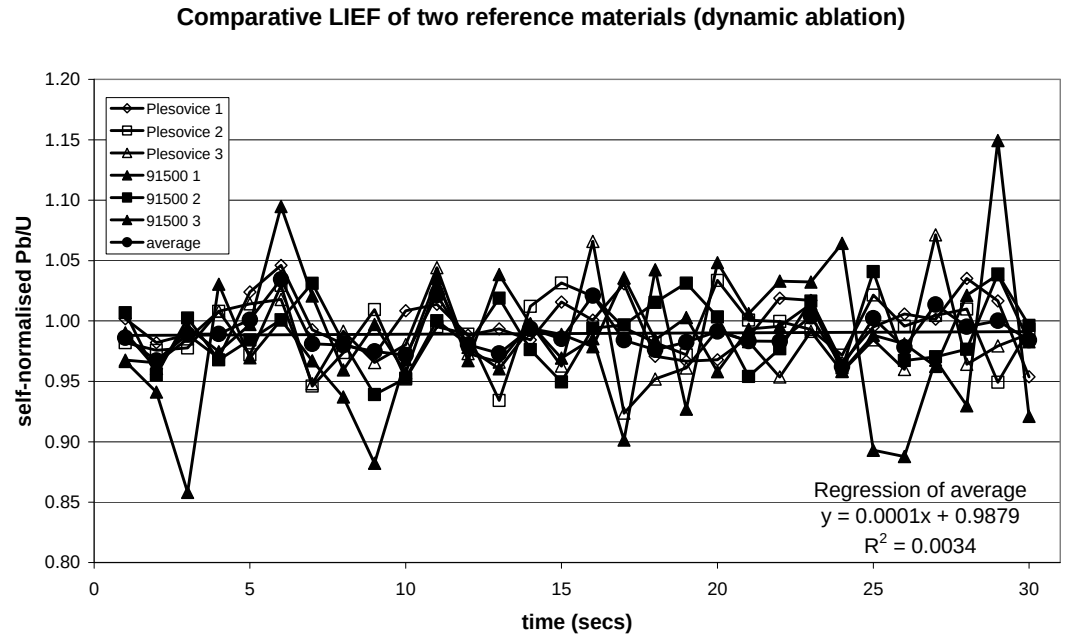

Figure 2a

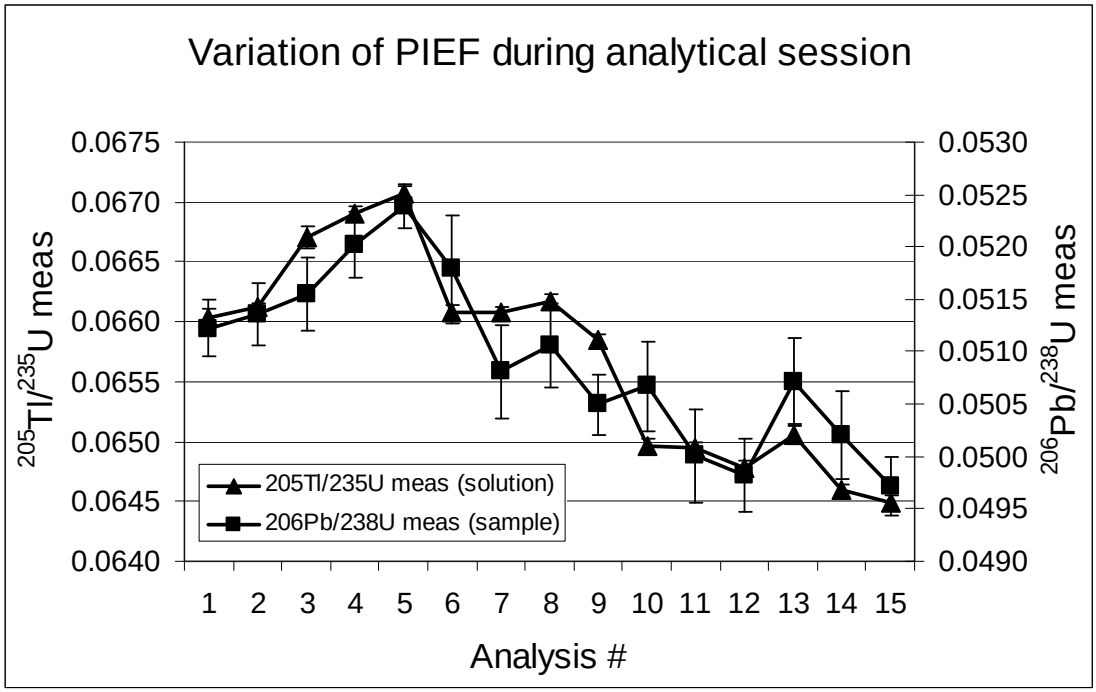

Figure 2b

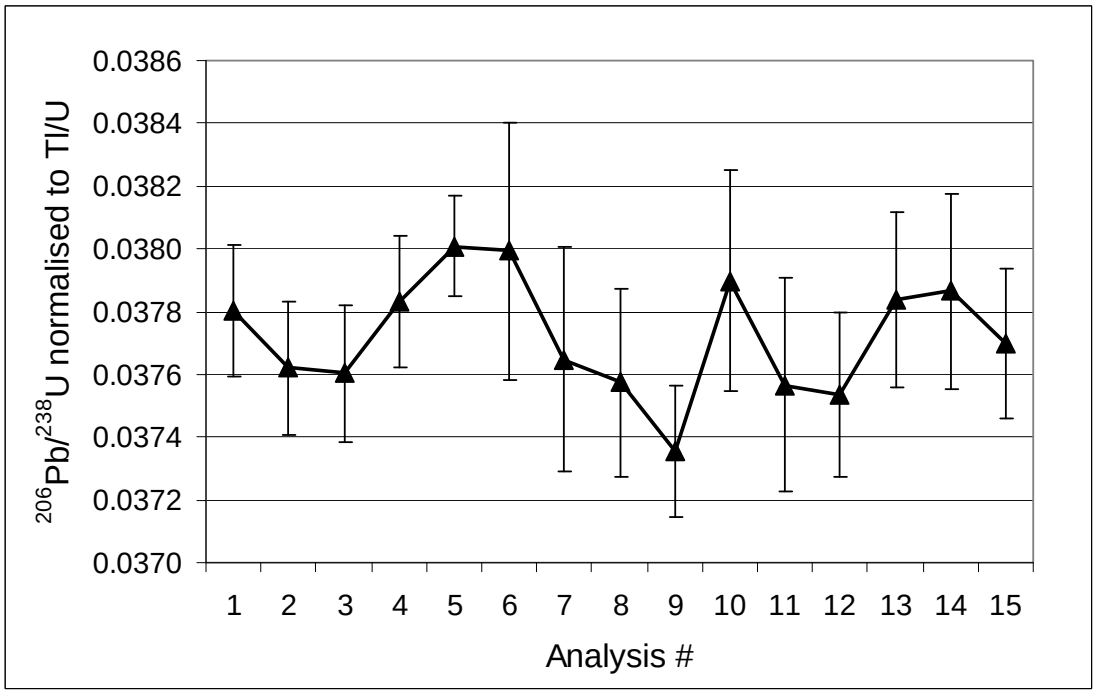

Figure 3a

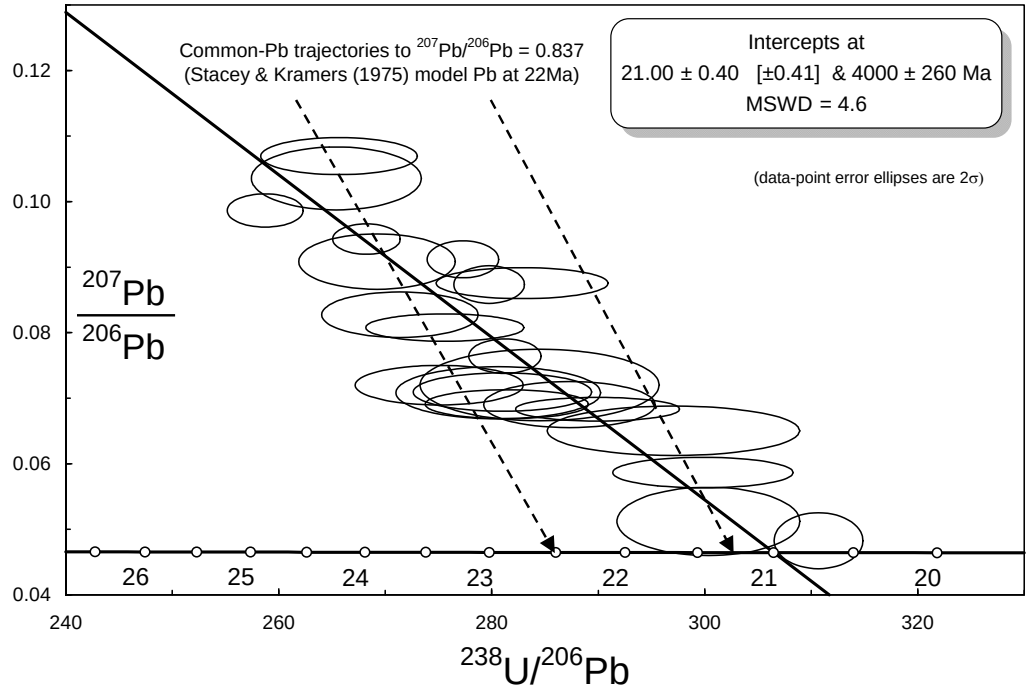

Figure 3b

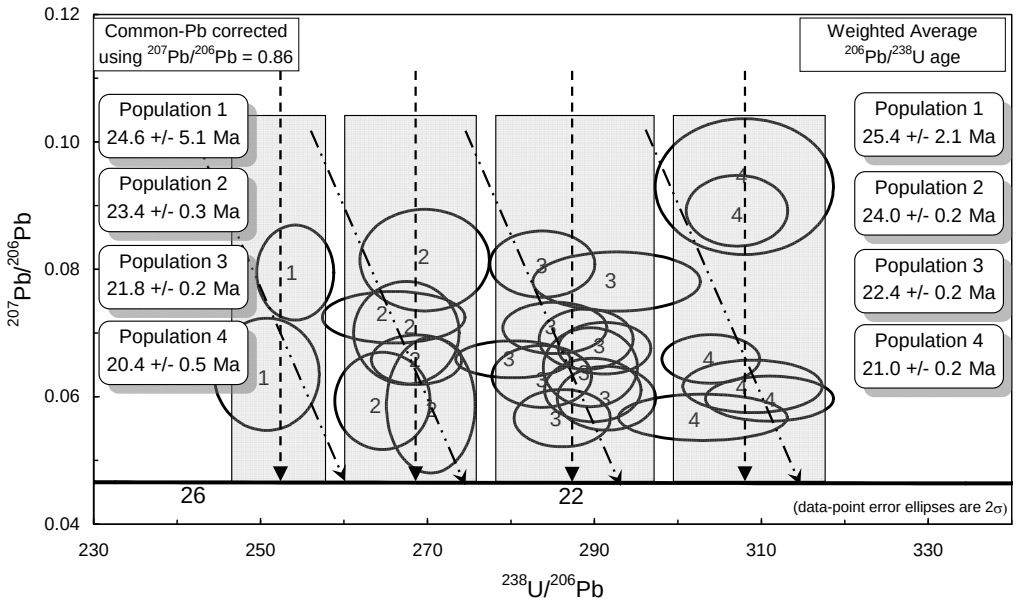

Figure 4

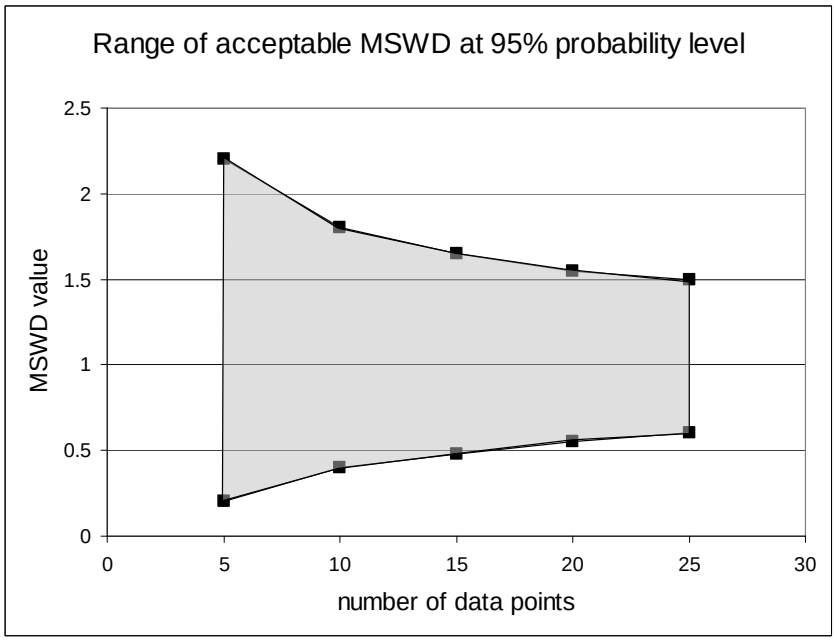

Figure 5

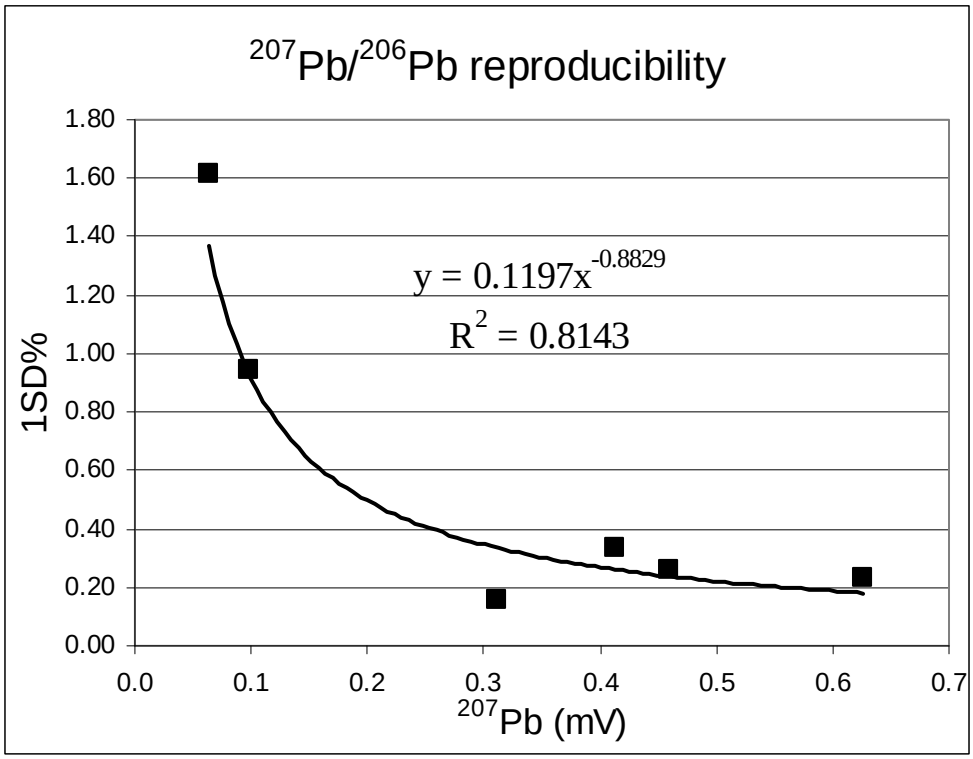

Figure 6a

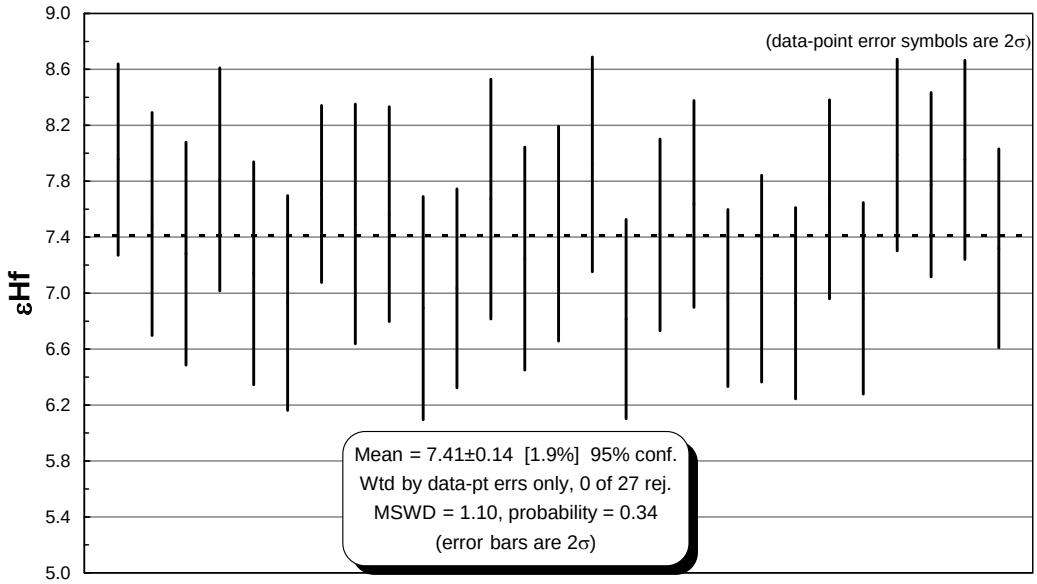
(data-point error symbols are 2σ)
εHf
9.0
8.6
8.2
7.8
7.4
7.0
6.6
6.2
5.8
5.4
5.0
Mean = 7.41±0.14 [1.9%] 95% conf.
Wtd by data-pt errs only, 0 of 27 rej.
MSWD = 1.10, probability = 0.34
(error bars are 2σ)

Figure 6b

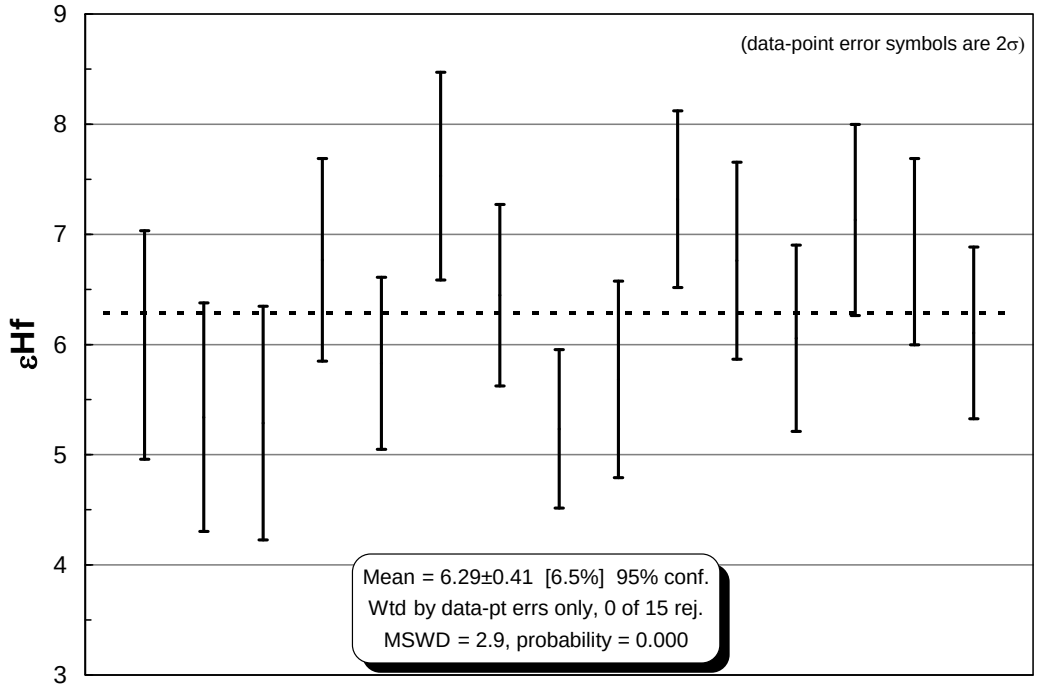
(data-point error symbols are 2σ)
εHf
9
8
7
6
5
4
3
Mean = 6.29±0.41 [6.5%] 95% conf.
Wtd by data-pt errs only, 0 of 15 rej.
MSWD = 2.9, probability = 0.000

Figure 7a

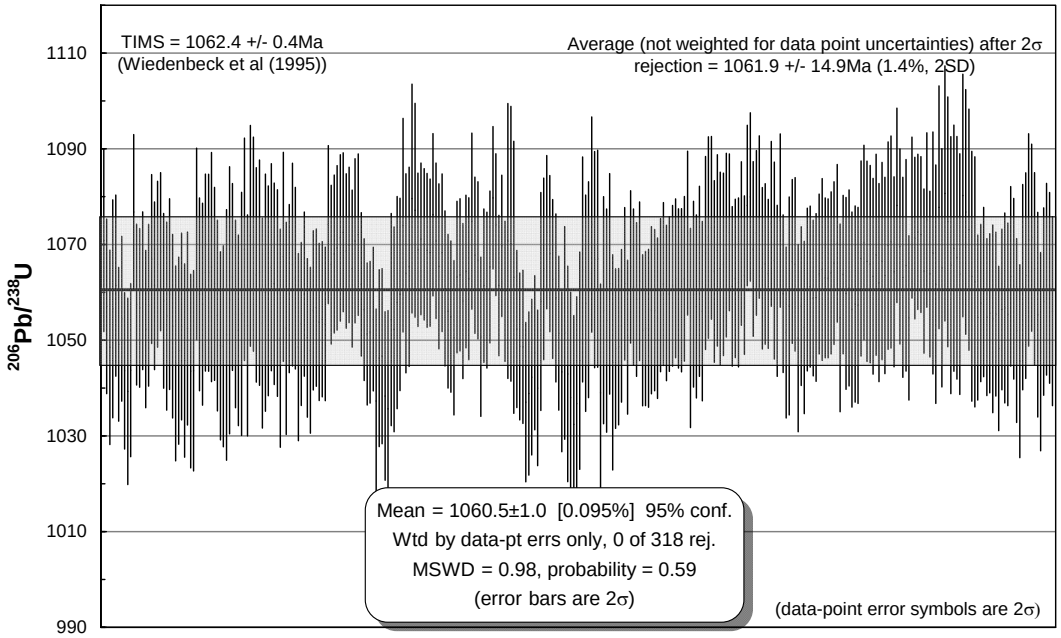

Figure 7b

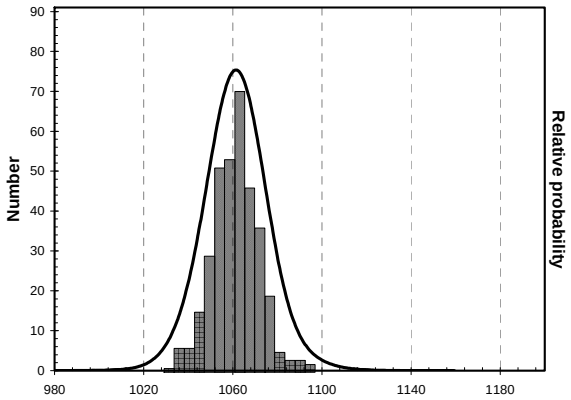

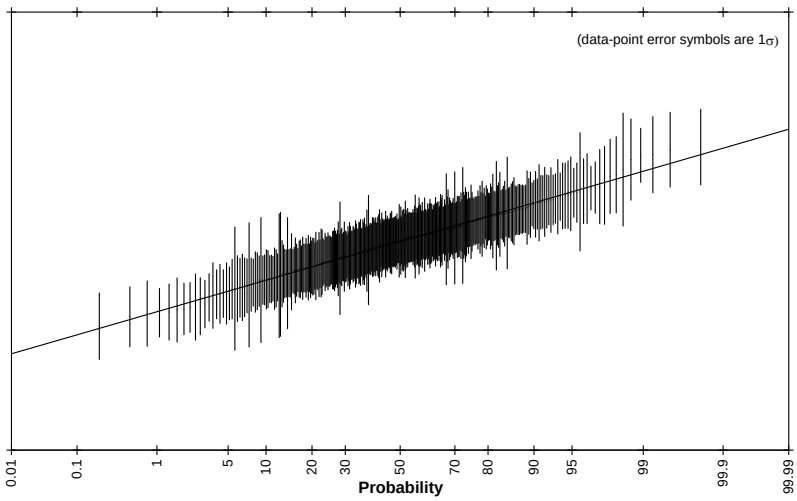

Figure 8

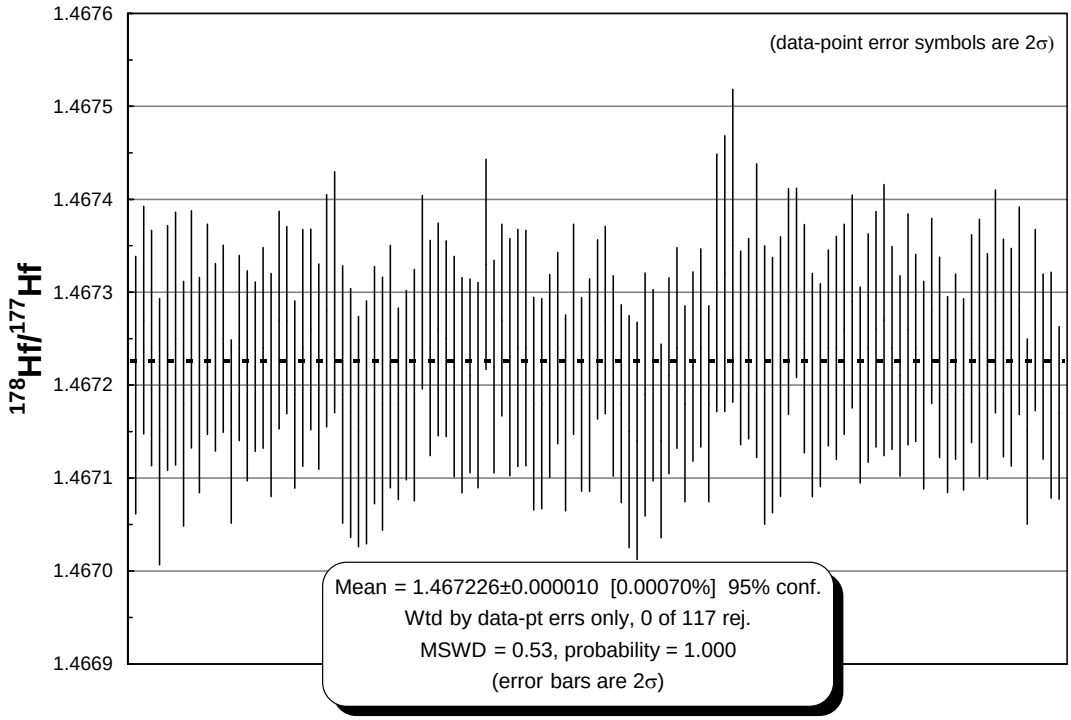

Figure 9

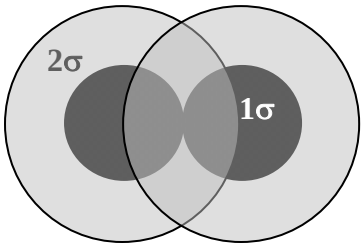

Figure 10a

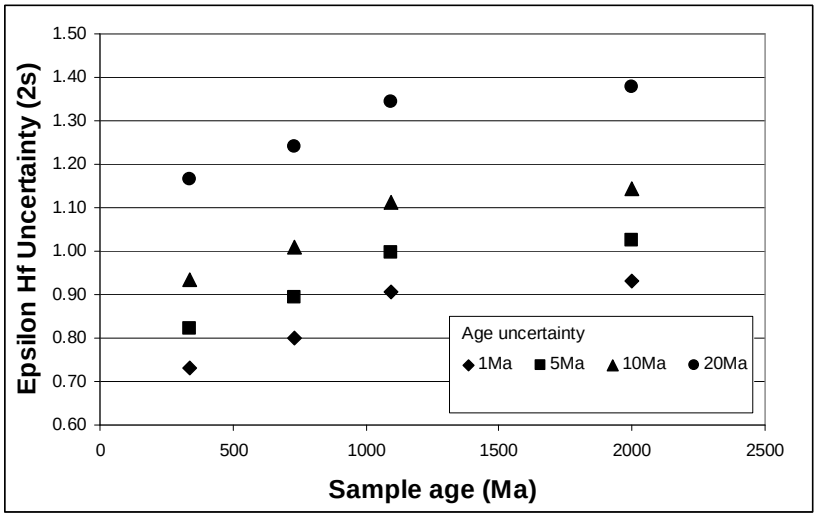

Figure 10b